Quasi Diabatic Representation for Nonadiabatic Dynamics Propagation

Arkajit Mandal,[†,‡] Sharma SRKC. Yamijala,[†,‡] and Pengfei Huo[*,†]

Department of Chemistry, University of Rochester, 120 Trustee Road, Rochester, New York 14627, United States

E-mail: pengfei.huo@rochester.edu

Model Hamiltonian and Parameters

Here we provide detailed expressions of all of model Hamiltonians used in the main text.

Tully's Model I[1]

$$\begin{aligned} V_{11}(R) &= A(1-e^{-BR}) \quad (\text{for} \quad R>0) \\ V_{11}(R) &= -A(1-e^{BR}) \quad (\text{for} \quad R<0) \\ V_{22}(R) &= -V_{11}(R) \\ V_{12}(R) &= V_{21}(R) = Ce^{-DR^2} \end{aligned} \tag{S1}$$

*To whom correspondence should be addressed

†Department of Chemistry, University of Rochester, 120 Trustee Road, Rochester, New York 14627, United States

‡A. M. and S. S. Y. contributed equally to this work.

Tully's Model II[1]

$$\begin{aligned} V_{11}(R) &= 0 \\ V_{22}(R) &= -Ae^{-BR^2} + E_0 \\ V_{12}(R) &= V_{21}(R) = Ce^{-DR^2} \end{aligned} \tag{S2}$$

Tully's Model III[1]

$$\begin{aligned} V_{11}(R) &= A \\ V_{22}(R) &= -A \\ V_{12}(R) &= Be^{CR} \quad (\text{for} \quad R < 0) \\ V_{12}(R) &= B(2 - e^{-CR}) \quad (\text{for} \quad R > 0) \end{aligned} \tag{S3}$$

The parameters (in a.u.) of the above three Tully's models are tabulated below.

model	A	B	C	D	E_0
I	0.01	1.6	0.005	1.0	-
II	0.1	0.28	0.015	0.06	0.05
III	6×10^{-4}	0.1	0.9	-	-

Morse Potential Models[2,3]

$$\begin{aligned} V_{ii}(R) &= D_i(1 - e^{-a_i(R-b_i)}) + E_i \\ V_{ij}(R) &= A_{ij}e^{-c_{ij}(R-d_{ij})^2} \\ V_{ij}(R) &= V_{ji}(R) \end{aligned} \tag{S4}$$

The parameters (in a.u.) for the three models used in the main text are tabulated below:

	Model I			Model II			Model III		
i	1	2	3	1	2	3	1	2	3
D_i	0.003	0.004	0.003	0.02	0.01	0.003	0.02	0.02	0.003
a_i	0.65	0.6	0.65	0.65	0.4	0.65	0.4	0.65	0.65
b_i	5.0	4.0	6.0	4.5	4.0	4.4	4.0	4.5	6.0
E_i	0.0	0.1	0.006	0.0	0.01	0.02	0.02	0.0	0.02
ij	12	13	23	12	13	23	12	13	23
A_{ij}	0.002	0.0	0.002	0.005	0.005	0.0	0.005	0.005	0.0
c_{ij}	16.0	0.0	16.0	32.0	32.0	0.0	32.0	32.0	0.0
d_{ij}	3.40	0.0	4.80	3.66	3.34	0.0	0.02	0.0	0.02

Conical intersection model

The total Hamiltonian for the conical intersection model[4] is given by

$$\hat{H} = \sum_j \frac{1}{2}\left[P_j^2 + \omega_j^2 R_j^2\right] + \sum_\alpha \left[E_\alpha + \sum_j c_j^\alpha R_j\right] |\alpha\rangle\langle\alpha| + \lambda R_{10a}\left[|1\rangle\langle 2| + |2\rangle\langle 1|\right], \qquad \text{(S5)}$$

where $R_j \in \{R_1,\, R_{6a},\, R_{10a}\}$.

The parameters (in eV) are tabulated below

i	E_i	c_1^i	c_{6a}^i	c_{10a}^i
1	3.94	0.037	-0.105	0
2	4.84	-0.254	0.149	0
	ω_1	ω_{6a}	ω_{10a}	λ
	0.126	0.074	0.118	0.262

7-state FMO complex

The total Hamiltonian for FMO complex[5] is given by :

$$\begin{aligned}
\hat{H} &= \hat{H}_{\mathrm{e}} + \hat{H}_{\mathrm{ep}} \\
\hat{H}_{\mathrm{e}} &= \sum_{\alpha} \epsilon_{\alpha} |\alpha\rangle\langle\alpha| + \sum_{\alpha \neq \gamma} \Delta_{\alpha,\gamma} |\alpha\rangle\langle\gamma| \\
\hat{H}_{\mathrm{ep}} &= \sum_{\alpha} \sum_{j_\alpha} [\frac{1}{2}(\hat{P}_{j_\alpha}^2 + \omega_{j_\alpha}^2 \hat{R}_{j_\alpha}^2) + c_{j_\alpha} \hat{R}_{j_\alpha} |\alpha\rangle\langle\alpha|]
\end{aligned} \tag{S6}$$

The electronic Hamiltonian ($\hat{H}_{\mathrm{e}}$) matrix (in cm^{-1}) in the diabatic basis is given by :

$$\hat{H}_e = \begin{bmatrix}
12410 & 87.7 & 5.5 & 5.9 & 6.7 & 13.7 & 9.9 \\
87.7 & 12530 & 30.8 & 8.2 & 0.7 & 11.8 & 4.3 \\
5.5 & 30.8 & 12210 & 53.5 & 2.2 & 9.6 & 6.0 \\
5.9 & 8.2 & 53.5 & 12320 & 70.7 & 717.0 & 63.3 \\
6.7 & 0.7 & 2.2 & 70.7 & 12480 & 81.1 & 1.3 \\
13.7 & 11.8 & 9.6 & 17.0 & 81.1 & 12630 & 39.7 \\
9.9 & 4.3 & 6.0 & 63.3 & 1.3 & 39.7 & 12440
\end{bmatrix} \tag{S7}$$

Bath Discretization Protocol of the Spin-Boson Model

The coupling parameters and the frequencies for the bath in the Spin-Boson are sampled based on the discretized spectral density

$$J(\omega) = \frac{\pi}{2} \sum_{i=1}^{N} \frac{c_i^2}{\omega_i} \delta(\omega - \omega_i) \tag{S8}$$

For spin-boson model, an Ohmic spectral density is used

$$J(\omega) = \frac{\pi}{2} \xi \omega e^{-\omega/\omega_c}, \tag{S9}$$

where ξ is the Kondo parameter, and ω_c is the cutoff frequency. The vibrational frequencies and the coupling coefficients are sampled[6] based on the following expressions

$$\omega_i = -\omega_c \ln\left(1 - i\frac{\omega_0}{\omega_c}\right) \tag{S10}$$

$$c_i = \sqrt{\xi\omega_0}\omega_i. \tag{S11}$$

Here, for a total of N bath modes, $\omega_0 = \frac{\omega_c}{N}\left(1 - e^{-\omega_{\rm m}/\omega_c}\right)$. In addition, $\omega_{\rm m}$ was chosen to be $3\omega_c$ for the model calculations.

Bath Discretization Protocol of the FMO Model

In the EET model Hamiltonian of the FMO complex,[5] each state is coupled to a set of independent oscillators. The system-bath couplings are characterized by the following Debye spectral density

$$J(\omega) = 2\lambda\frac{\omega\tau}{1+\omega^2\tau^2}, \tag{S12}$$

where λ is reorganization energy, and τ is the solvent response time.

The vibrational frequencies and the coupling coefficients are sampled based on the following expressions[7]

$$\omega_j = \tan\left(\frac{j}{N}\tan^{-1}(\omega_m\tau)\right) \tag{S13}$$

$$c_j = 2\omega_j\sqrt{\frac{\lambda}{\pi N}\tan^{-1}(\omega_m\tau)} \tag{S14}$$

where N is the total number of bath DOF. Here, $\omega_{\rm m}$ was chosen to be $20/\tau$.

Validating the MO truncation scheme

Here, we provide the results to validate the truncation scheme used in the main text for propagating TDSE. Fig. S1A presents the time-dependent energies of both active space MOs (colored lines) and the MOs adjacent to them (black lines). One can clearly see that the other MOs are energetically separated from the LUMO to LUMO+9 active space MOs, with a gap that is at least 0.5 eV. As a consequence, the numerical solutions of TDSE in the active space should be exactly the same compared to those using the entire set of MOs, when the initial conditions are also in the same active space. Fig. S1B presents the numerical solutions of TDSE (see Appendix A of the main text) with the active space (open circles) and with the entire set of MOs (solid lines), which are numerically indistinguishable.

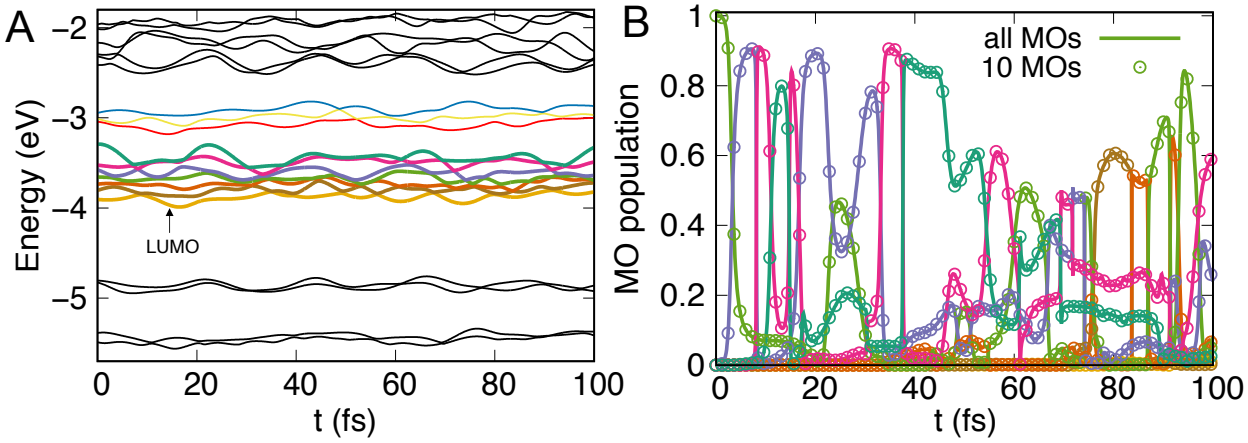

Figure S1: (A) Time-dependent MO energies near the active space in the $2H_2Pc/C_{60}$ model system. The active space, LUMO to LUMO+9, is depicted with colored MOs. (B) Time-dependent adiabatic populations of the LUMO to LUMO+6 MOs. Results are obtained by solving TDSE with the entire set of MOs (solid lines) or only with the active MOs (open circles).

References

(1) Tully, J. C. Molecular dynamics with Electronic Transitions. *J. Chem. Phys.* **1990**, *93*, 1061–1071.

(2) Coronado, E. A.; Xing, J.; Miller, W. H. Ultrafast Non-Adiabatic Dynamics of Systems With Multiple Surface Crossings: A Test of the Meyer-Miller Hamiltonian with Semiclassical Initial Value Representation Methods. *Chem. Phys. Lett.* **2001**, *349*, 521–529.

(3) Duke, J. R.; Ananth, N. Simulating Excited State Dynamics in Systems with Multiple Avoided Crossings Using Mapping Variable Ring Polymer Molecular Dynamics. *J. Phys. Chem. Lett.* **2015**, *6*, 4219–4223.

(4) Stock, G.; Thoss, M. *Conical Intersections*; 2011; pp 619–695.

(5) Ishizaki, A.; Fleming, G. R. Theoretical Examination of Quantum Coherence in a Photosynthetic System at Physiological Temperature. *Proc. Nat. Acad. Sci. U.S.A.* **2009**, *106*, 17255âĂŞ17260.

(6) Makri, N. The Linear Response Approximation and its Lowest Order Corrections: An Influence Functional Approach. *J. Phys. Chem. B* **1999**, *103*, 2823–2829.

(7) Huo, P.; Coker, D. F. Semi-Classical Path Integral Non-Adiabatic Dynamics: A Partial Linearized Classical Mapping Hamiltonian Approach. *Mol. Phys.* **2012**, *110*, 1035–1052.